nature communications

Article

https://doi.org/10.1038/s41467-026-69850-x

Radiolabeling of oligopeptides by selective hydrogen isotope exchange with deuterium and tritium in aqueous buffers

Received: 4 September 2025

Accepted: 11 February 2026

Published online: 07 March 2026

Check for updates

Elisa Martinelli[1,2], Remo Weck[1], Stefan Güssregen[3] & Volker Derdau[1]

Isotopic labeling of organic compounds is crucial for advancements in life sciences and is extensively utilized in drug discovery. While isotopic labeling is widely applied to small molecules, research on isotopically labeled biologics such as peptides, antibodies, or enzymes remains less developed, despite the increasing prevalence of these larger biologics in the pharmaceutical industry as transformative treatments for patients. We report the development of an in situ prepared catalyst for Hydrogen Isotope Exchange reactions with deuterium or tritium gas as the isotope source to selectively label peptides in aqueous solutions. The method requires only low amounts of catalyst and provides the radiolabeled peptide in a single reaction step with sufficient specific activity for biological in-vitro experiments, paving the way for future developments and applications in biological based drugs studies. Furthermore, we have identified a substrate-mediated formation of the active catalytic species, leading to the high selectivity in this late-stage functionalization approach of complex peptide compounds. DFT calculations and NMR studies have identified the intermediate species involved. The reported insights accelerate the access to radiolabeled tracers to understand biological processes, as well as offer future opportunities for highly selective C-H activation and C-C or C-X bond formation to achieve highly selective late-stage functionalization products.

Isotopic labeling of organic compounds remains critical for advancements in life sciences and is heavily utilized in drug discovery, agricultural science, and medical imaging[1–4]. Replacing a common isotope with a rare or radioactive counterpart enables scientists to trace biological pathways and processes through mass spectrometry or radiation detection[5,6]. Although isotope labeling is common for small active pharmaceutical ingredients, studies on isotopically labeled biologics are not as advanced[7,8], despite these larger biologics becoming increasingly prevalent in the pharmaceutical industry as life changing treatment for patients[9]. The reported methods to synthesize isotopically labeled antibodies, peptides, proteins, polysaccharides, and RNAs are notably sparse and are either resource intensive or based on conjugation chemistry[10]. Bypassing the requirement for lengthy multiple step syntheses, Hydrogen Isotope Exchange (HIE)[11–21], considered as the most basic form of C-H functionalizations[22–26], has emerged as a common method for introducing deuterium or tritium into complex molecules. While HIE methods for small molecules typically target aromatic structures, aliphatic C-H positions[27] common in biologics remain challenging, particularly for selective labeling in aqueous buffers[28,29]. Strategic isotopic placement is crucial as hydrogen's involvement in all metabolic processes[30] increases the risk of losing tritium labels compared to carbon-14. For this reason, methods targeting inactivated C-H positions are valuable for creating tritium tracers with broader applications in life sciences, especially for in vivo experiments.

[1]Sanofi Germany, R&D, Integrated Drug Discovery, Isotope Chemistry, Industriepark Höchst, Frankfurt, Germany. [2]Leibniz-Institut für Katalyse e. V., Albert-Einstein-Str. 29a, Rostock, Germany. [3]Sanofi Germany, R&D, Integrated Drug Discovery, Synthetic Molecular Design, Industriepark Höchst, Frankfurt, Germany. e-mail: volker.derdau@sanofi.com

Over the past decade, numerous research teams have reported significant advancements in HIE labeling by incorporating deuterium into amino acids and peptides (Fig. 1A). There was limited success or evidence in adapting these methods to tritium applications. Early HIE deuteration methods utilized strongly acidic conditions; in 2013 for example, Hashimoto developed a method for HIE on aromatic α-amino acids and related peptides using deuterated trifluoromethanesulfonic acid (TfOD)[31]. The process showed consistent hydrogen/deuterium substitution with retention of stereochemistry for phenylalanine for all aromatic C-H positions, while tyrosine exhibited specific substitution at the *ortho*-C-H sites of its phenol component. Recently, Kim reported the enantionselective deuteration of α-amino acids by base catalysis using only sodium ethoxide (NaOEt) in deuterated ethanol (EtOD) and no external chiral source. The protocol is especially noteworthy because it shows chirality retention on optically active α-amino acid derivatives when α-deuteration is obtained in protic solvents[32]. In 2015, Pieters devised a selective heterogeneous catalyzed method for enantiospecific C(sp^3)-H bond activation and subsequent deuteration, utilizing deuterium gas as the deuterium source and heterogeneous RuPVP coated nanoparticles as catalysts[33]. The fully stereoretentive HIE was observed selectively only at the C-H α-position of primary amine moieties. Even though no protecting groups were applied, the reaction could not be transferred to tritium conditions. Ligated iridium and ruthenium nanoparticles were reported by Chaudret and Lippens to deuterate L-lysine predominantly at the α-nitrogen positions[34,35]. In this context Roche reported similar selectivity in a scalable method for the stereoretentive deuteration of amino acids and amines at C-H-α amino positions applying Ru/C and deuterium oxide (D_2O)[36]. An eco-friendly Pd/C-Al-D_2O catalytic system for the chemo/regioselective H/D exchange of amino acids was showcased by Török in 2022. This method leverages the in situ generation of D_2 gas through aluminum and D_2O interaction and the palladium catalyst facilitating the reaction[37]. Gunanathan applied the homogeneous catalyst monohydrido-bridged ruthenium complex [{(η^6-pcymene) RuCl}$_2$(μ-H-μ-Cl)] in selective HIE of primary and secondary α-amines, amino acids, and drug molecules using D_2O as deuterium source[38]. Takeda,

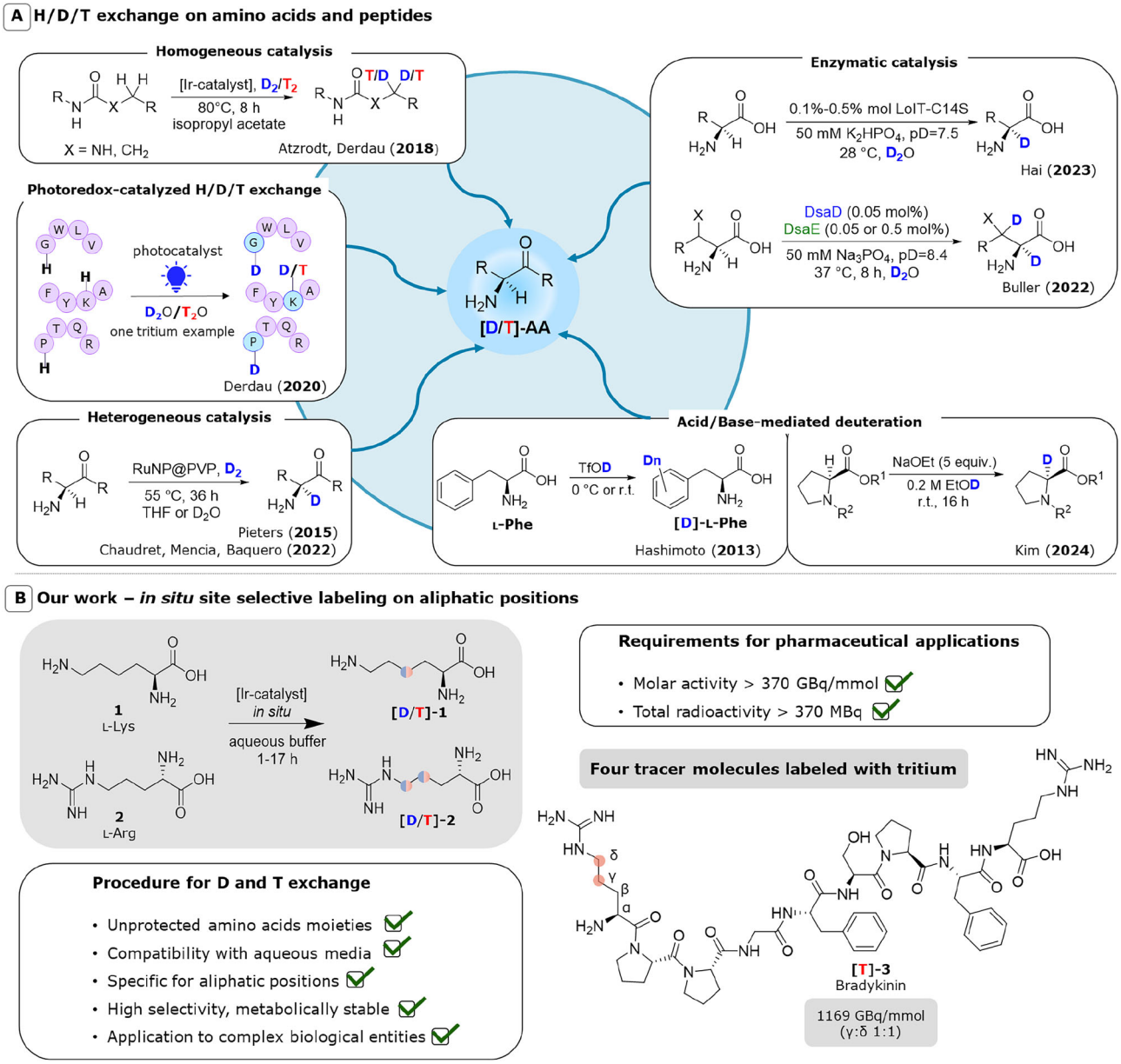

Fig. 1 | HIE applied to amino acids. A representative methods for HIE applied to amino acids. **B** selective HIE labeling of unprotected amino acids on aliphatic positions and its application to tritium labeling of peptides in buffer, red/blue dot = isotope labeling position.

Moriwaki, and Soloshonok enhanced the method by achieving enantioconvergent deuteration of amino acids using a chiral nickel complex via dynamic kinetic resolution and MeOH-d_4 as an isotope source. With the appropriate choice of ligand configuration, the α-deuterated amino acids could be synthesized in both L- and D-enantiomers. However, a significant constraint of this approach is the need for stoichiometric amounts of the chiral nickel complex, where the deuterated products are released after being treated with hydrochloric acid[39]. In 2018 Atzrodt and Derdau demonstrated the use of iridium(I)-catalyst in HIE of aliphatic C-H positions of protected amino acids and smaller peptides with up to four amino acids[40]. The method was transferred to tritium, with protected amino acids and aprotic, organic solvents were used at elevated temperatures. In 2017 the MacMillan group reported the direct installation of deuterium or tritium at α-amino C(sp^3)-H bonds by a photoredox-mediated hydrogen atom transfer (HAT) protocol utilizing an iridium(III)photo-catalyst and D_2O/T_2O as isotope sources under mild conditions (room temperature)[41]. While the initial report focused on tertiary amines, Derdau could extend the conditions to primary and secondary amines including amino acids by modifying the base and reported one tritium reaction with L-lysine with THO as the isotope source[42]. Recently, enzyme catalysis was applied to selectively achieve a racemization-free α-deuteration of L-amino esters by using a pyridoxal phosphate (PLP)-dependent enzyme (SxtA AONS)[43]. In 2023, Hai discovered that PLP Mannich Cyclase has shown proficiency in incorporating deuterium in the alpha-position of various L-amino acids applying D_2O as D-source[44]. Moreover, Buller reported the site-selective deuteration of amino acids using a dual-protein catalytic system. Interestingly, an aminotransferase (DsaD) can be used in combination with a small partner protein (DsaE) to obtain H/D exchange on the C-H α- and C-H β -positions of amino acids, while reactions that involve only DsaD yield exclusively Cα-deuteration[45]. In selective HIE conditions, the catalyst typically coordinates with a heteroatom like nitrogen or oxygen, making most HIE methods adjacent to the amine group. Even though there are already significant advances in the field, there is currently no selective method in buffers for deuteration or tritiation of unprotected amino acids or peptides which is needed for preparation of radiotracer biologics in a single reaction step in aqueous media. In this work we report a method for selective HIE reactions on unprotected amino acids and oligopeptides by the formation of in situ catalytic system using D_2 and T_2 gas as isotope sources. Mechanistic investigations were experimentally initiated and assisted by DFT calculations, revealing a complex path leading to the formation of the active species and the consequent selective labeling on the aliphatic C-H positions.

Results and Discussion

We started our search for a catalytic system for aliphatic C-H positions by testing various metal precursors and ligands in an HIE reaction with a 2-piperidyl-pyrimidine derivative **4** in water, using D_2 as the D-source, at 90 °C (Fig. 2A). The groundwork for our research stemmed from earlier studies on aliphatic HIE in organic solvents[46] and aromatic HIE in water[28,29]. We were delighted to discover that our modular in situ approach[47,48], employing various transition metal pre-catalysts along with nitrogen, phosphorus, or carbene ligands, was able to generate an active HIE catalyst producing promising results with deuteration at C(sp^3) positions in aqueous buffers. While the in situ formed catalytic systems, comparable to iridium(I) catalysts reported by Crabtree[49], Kerr[50–66] or Heys[67–72], resulted only in low aliphatic deuterations under the tested reaction conditions, we found a significant HIE activity for iridium cyclooctadiene (COD) pre-catalysts, $[Ir(COD)Cl]_2$ or $[Ir(COD)(OMe)]_2$ with phosphine ligand **L5** and rhodium pre-catalyst $[Rh(COD)OH]_2$ with NHC carbene ligand **L3** (Fig. 2A). Even though iridium and rhodium catalysts showed both significant HIE for the model substrate **4**, we also observed saturation of the pyrimidine ring under rhodium catalysis (Figure S10, page 14 of Supplementary Information). Nevertheless, we decided to screen substrate specificity of the rhodium pre-catalyst with NHC carbene **L3** and both iridium pre-catalysts with phosphine ligand **L5** against five different amino acids **AAs** such as lysine (basic), histidine (aromatic, basic), glutamic acid (acidic), serine (neutral), and tryptophane (neutral, aromatic). We were interested to see if our discovered C(sp^3)-HIE activity could be transferred to monomeric building blocks of biologicals (Fig. 2B). While we found no HIE product for most tested amino acids, we observed deuterium incorporation in L-lysine **1** with 1.1 D/molecule. In the next optimization round, we screened 15 different phosphine ligands **L5-L19** in the HIE reaction of L-lysine **1** in a 1:2 ratio with pre-catalyst $[Ir(COD)Cl]_2$ in pH 9 borax buffer at 90 °C (Fig. 2C). We found that tris-(*ortho*-methoxyphenyl)phosphine **L11** showed the best results and increased the deuterium incorporation to 1.5 D/molecule. Finally, we further examined reaction parameters such as time, catalyst loading, phosphine equivalents or temperature (Section 4, pages 17–25 of Supplementary Information) and optimized the conditions to reach 1.7 D/molecule for L-lysine **1**. We observed that all parameters are crucial for the success of the reaction. Prolonging of the reaction time over 60 min or higher amounts of catalyst loading than 2.5 mol% yielded a significant decrease of deuterium content in the product. When the amount of the catalyst was increased to 7.5 mol% the formation of less reactive metal clusters was detected (Table S7, page 19 of Supplementary Information). While it is described that in organic media these metal particles precipitate with pre-catalyst $[Ir(COD)Cl]_2$[73] or $[Ir(COD)(OMe)]_2$[74] under reductive conditions (H_2/D_2) within seconds, this process is inhibited in low catalyst concentrations in the presence of the lysine substrate in water. We concluded that without the stabilization of the metal complex due to the substrate, metal particles were likely formed, which are known to catalyze side reactions with water that decrease the amount of deuterium in the gas phase[75].

As optimized HIE conditions we identified for 0.02 mmol scale lysine substrate: 2.5 mol% $[Ir(COD)Cl]_2$, 5 mol% phosphine **L11**, 100 equiv. D_2, 3 mL of Borax/HCl buffer pH 9, 90 °C, 1 h.

Interestingly, proton and deuterium NMR studies disclosed a unique label position for lysine at the γ-CH_2 group. As this HIE selectivity for iridium(I) catalysis was surprising, it triggered further experiments to understand the reactivity and the reaction mechanism. Experimentally we examined HIE reactions with simplified analogs based on lysine (Fig. 3A). Amino- or/and carboxylic-substituted mono- and di-functionalized hydrocarbons were tested. Mono-functionalized compound **12** showed no HIE activity at all, indicating the need for two functional groups. Diamines **13-14** gave selective deuteration in the γ-position with 1.0–1.1 D/molecule. The HIE reaction with 6-aminopentanoic acid **15** showed a significant decrease in deuterium incorporation (0.2 D/molecule) compared to lysine **1** and diamines **13-14**. Cyclic diamines such as compound **17** resulted in decreased deuterium incorporation as well. Interested by the obtained result with compound **17**, used as mixture of cis- and trans-isomers, we explored the reaction outcome when the pure **17-cis** and **17-trans** isomers were used. Only compound **17-cis** was deuterated in the reaction conditions (Figures S52–S55, pages 57–60 of Supplementary Information), showing the need of having both amino-groups on the same side of the plane represented by the cyclic core of the molecule. Enlargement of the carbon chain by one carbon yielded the HIE product **18** with deuterium in both the 3- and 4-position. Interestingly, diamine **9** with four carbons in the chain resulted the HIE product with deuterium at all C-positions. No deuterated product was observed for prolongated chains of seven (**19**) or eight (**20**) carbons. Besides lysine **1**, we also found arginine **2** as suitable substrate under the HIE reaction conditions, however with lower deuterium incorporation of 0.8 D/molecule and a slightly changed selectivity, resulting in a 1:1 ration between positions γ and δ. Amidine **10** was selectively deuterated on one position resulting in 0.2 D/molecule. Interestingly, when the amine moiety was substituted with a carboxylic acid (**11**), no deuterium incorporation was obtained.

https://doi.org/10.1038/s41467-026-69850-x

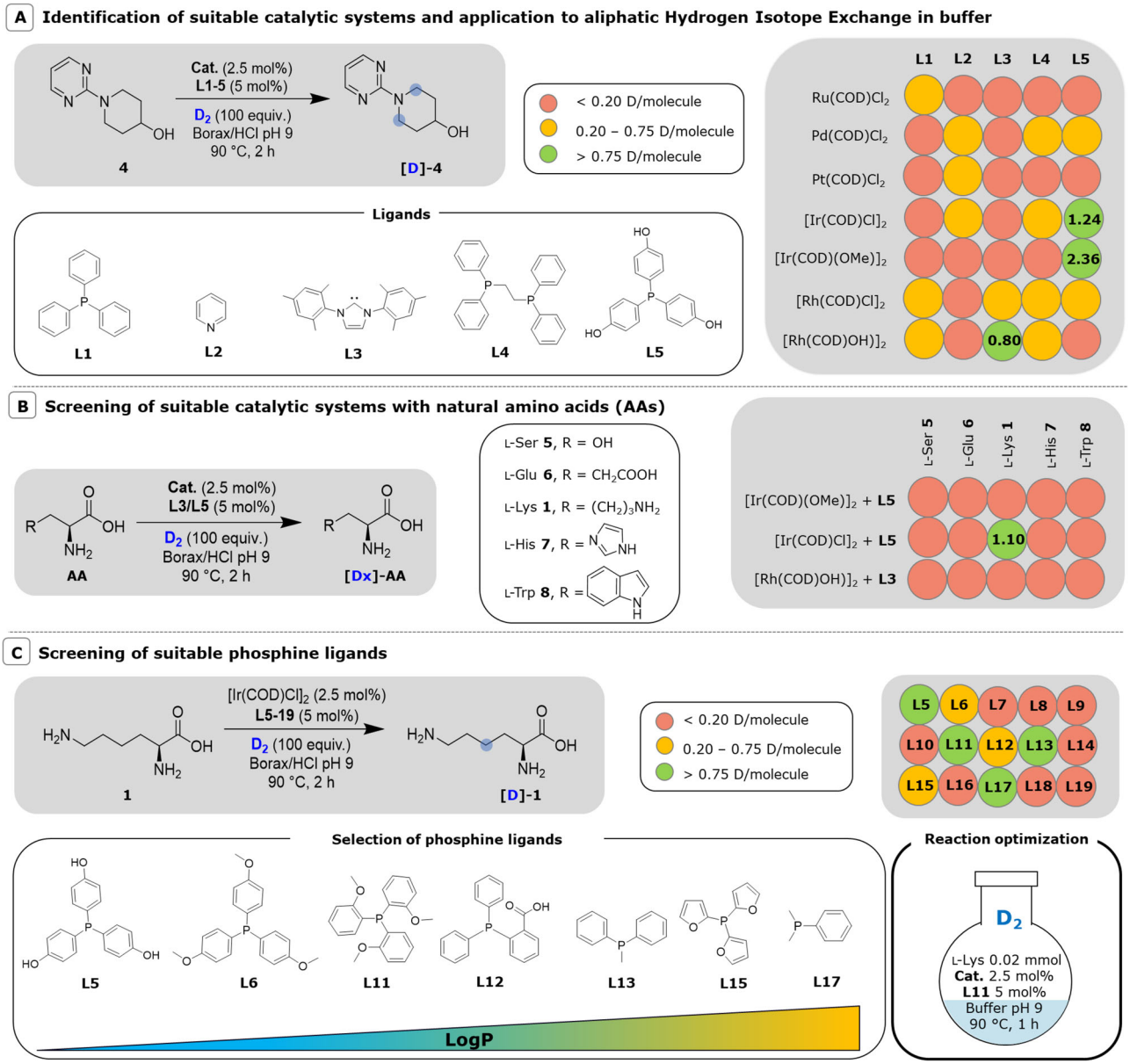

Fig. 2 | Reaction optimization. A catalyst system identification; **B** screening of identified catalytic systems with different amino acids; **C** phosphine ligands screening. General conditions: 0.02 mmol substrate, 2.5 mol% pre-catalyst (**Cat.**), 5 mol% ligand, Borax/HCl buffer pH 9, 90 °C, 2 h. Deuterium content analyzed by LC-MS. Color coding: red for <0.20 D/molecule, orange 0.20–0.75 D/molecule, green > 0.75 D/molecule. LogP chart: from less (blue) to more lipophilic (yellow); blue dot = deuterium labeling position.

The unexpected experimental results triggered intensive theoretical investigations using Density Functional Theory (DFT) calculations where a great number of plausible intermediate species were investigated in terms of their thermodynamic profile within a reaction network. For this, we applied the M06-2X level of theory which provides good accuracy for thermochemistry and kinetics at reasonable computational cost[76].

Interestingly, only $[Ir(COD)Cl]_2$ instead of $[Ir(COD)OMe]_2$ was leading to the deuterated product. Calculations indicated that the different results are due to different energetics of the breakdown of the dimeric complex in water. We found the breakdown to be mildly endergonic (ΔG_r = +3.3 kcal/mol) for $[Ir(COD)Cl]_2$, while it was strongly endergonic (ΔG_r = +23.1 kcal/mol) for $[Ir(COD)OMe]_2$. These unexpected findings provide an explanation for the different experimentally obtained HIE outcomes. Within the reaction conditions used, different pathways can happen simultaneously leading to a complex reactivity network for the active species formation. However, the success of the selective HIE reaction is attributed to the stabilization of the iridium species by the substrate at room temperature and throughout the catalytic cycle at elevated temperatures. The excess substrate ensures coordination, preventing catalyst inactivation or nanoparticle formation. Notably, calculations indicate that the phosphine ligand is not essential for stabilization post-COD hydrogenation, as coordination with two or more substrates provides similar complexation energies. However, the phosphine ligand is critical for facilitating HIE during the C-H pincer insertion product step. As well, the *ortho*-methoxy substituent could facilitate the exchange of water and substrate at the ligand sphere of the catalyst due to supporting polar interactions between the methoxy group and positively polarized hydrogens of water and substrate molecules.

Based on the experimental results and the DFT calculations we propose the following mechanism for the formation of the catalytic active species (Fig. 3B). Upon introduction of the $[Ir(COD)Cl]_2$ pre-

https://doi.org/10.1038/s41467-026-69850-x

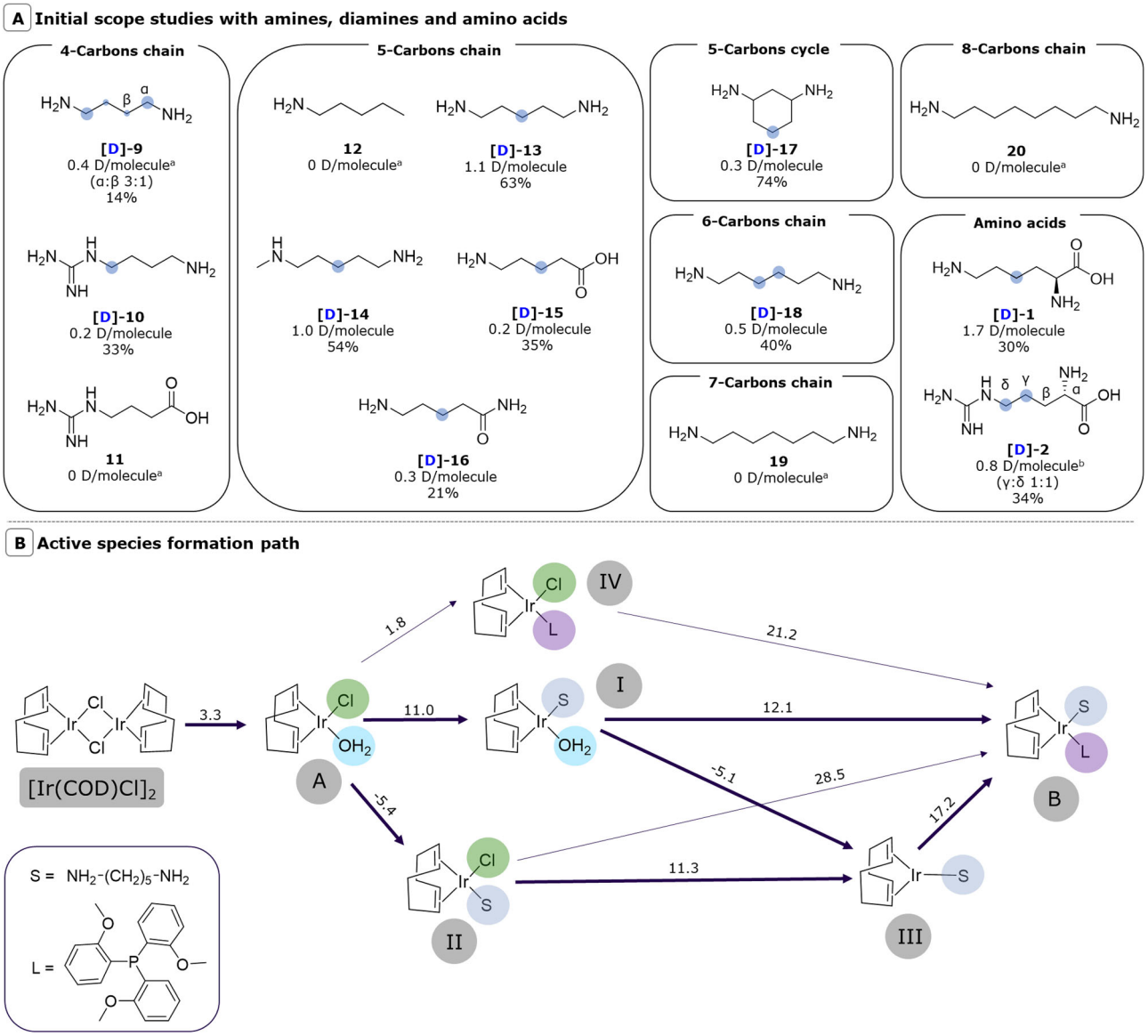

Fig. 3 | Mechanistic studies. A initial scope of deuteration with functionalized hydrocarbons and amino acids (blue dot = deuterium). Conditions: 0.02 mmol substrate, 2.5 mol% $[Ir(COD)Cl]_2$, 5 mol% ligand **L11**, Borax/HCl buffer pH 9, 90 °C, 1 h when not indicated otherwise. Deuterium content analyzed by ^{1}H-NMR when not indicated otherwise. Yield obtained with quantitative NMR. a) deuterium content analyzed by LC-MS; b) conditions for L-Arg: 0.02 mmol substrate, 5 mol% $[Ir(COD)Cl]_2$, 10 mol% ligand **L11**, Borax/HCl buffer pH 9, 90 °C, 17 h; (**B**) DFT calculations for the pathways leading to the active species formation. Reaction free energies ΔG_r (kcal/mol) are given above the corresponding reaction arrows, most energetically favorable pathways are represented with thick arrows.

catalyst in the aqueous solution at pH 9, the iridium atom coordinates with the one molecule of water, breaking the dimeric complex and forming complex **A** in a mildly endergonic step (ΔG_r = +3.3 kcal/mol). From the resulting complex **A**, heating up to 90 °C promotes that substrate and ligands compete at the Ir(I)-center giving rise to multiple reaction paths leading to d^8 square planar Ir(I) complexes with COD and up to two ligands and/or substrates. We found an energetically reasonable path where in a first endergonic step (ΔG_r = +11.0 kcal/mol) chlorine is replaced by the substrate (**I**), in this case represented as compound **13**, to form a *N*-coordination with the iridium atom. Subsequently, an endergonic displacement of water by one ligand molecule leads to the active species **B** (ΔG_r = +12.1 kcal/mol). However, it cannot be ruled out that other pathways leading to **B** can simultaneously occur through the formation of different intermediates (**II, III, IV**). The postulated mechanism upon addition of D_2 gas (Fig. 4A) starts with the reduction of the COD and the direct coordination of the iridium atom with deuterium and two additional molecules of water (**C**). This is an exergonic reaction (ΔG_r = −10.5 kcal/mol) to form a d^{10} octahedral complex as observed in earlier studies[28,29]. At the same time, heating at 90 °C promotes the displacement of one molecule of solvent by another substrate molecule (**D**) (ΔG_r = −0.8 kcal/mol), which is removed from the complex due to a bidentate coordination between the iridium metal and the two amino groups of the same substrate molecule (**E**) in an exergonic fashion (ΔG_r = −0.7 kcal/mol). Upon loss of one molecule of water, the coordination complex (**F**) is formed in an exergonic process (ΔG_r = −4.1 kcal/mol). This is followed by the formation of the CH insertion product (**G**) where the iridium is coordinated with both the γ carbon atom on the molecule and its C-H bond. Overall, the formation of the CH insertion product (**G**) on the energetically favorable γ position is obtained in an endergonic step (ΔG_r = +13.7 kcal/mol), representing the rate determining step of the catalytic cycle. Successive H/D exchange yields intermediate **H** (ΔG_r = −0.1 kcal/mol). The H/D exchange that occurs between the insertion products **G** and **H** is due to the fluxionality of the dihydrogen

https://doi.org/10.1038/s41467-026-69850-x

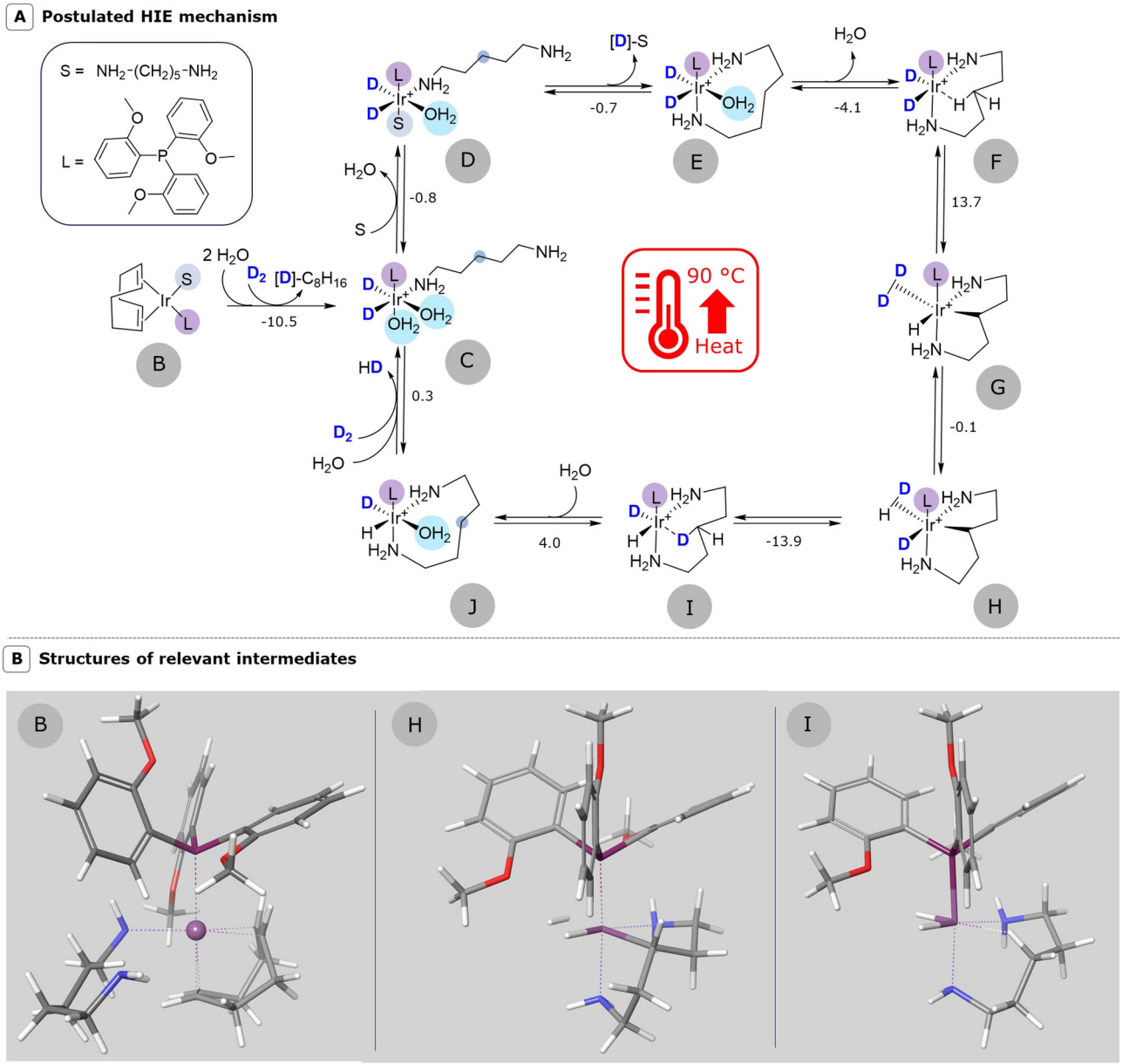

Fig. 4 | Postulated mechanism. A Postulated HIE mechanism upon introduction of D_2 and heating at 90 °C. The numbers below the arrows stand for the calculated energy ΔG_r (kcal/mol); (**B**) Structures of intermediate complexes involved in the H/D exchange. Blue dot = deuterium labeling position.

hydride that allows he cis-position orientation of the isotopic hydrogen in relation to the Ir–C bond[58 77]. This complex then undergoes C – D bond formation, obtaining coordination complex **I**, with the introduction of the deuterium atom on the molecule. Upon rehydration, complex **J** is generated (ΔG_r = 4.0 kcal/mol), maintaining the bidentate coordination of the iridium with the labeled substrate. Liberation of HD gas and introduction of water and D_2 gas leads to the regeneration of active complex **C** (ΔG_r = +0.3 kcal/mol), being coordinated to only one molecule of substrate and ready to start the cycle again. The release of the labeled compound is not immediate and is subordinated to the formation of the bidentate complex **E**. The significance of the pincer-type CH insertion products **G** and **H** is further supported by our investigations into alternative insertion pathways. We examined reaction paths via single-dentate insertion products, as well as insertion products without ligands and with two ligands. In all cases, the reaction energies for these alternative CH insertion products were higher than those in our proposed mechanism.

DFT calculations were conducted for the insertion step for each of the carbon atoms in the model compound to explain the selectivity in deuteration (Section 11.8, page 189 of Supplementary Information). Although the reaction energies for iridium insertion into the CH bond in the alpha, beta, or gamma positions were strongly positive, the lowest barrier was identified at the gamma position with ΔG_r = +9.4 kcal/mol. Despite heating the reaction mixture to 90 °C, the energy was insufficient to enable deuteration at the alpha and beta positions, respectively. For diaminobutane **9** or diaminohexane **18**, selectivity was partially lost due to ring strain in the chelation complex either simplifying coordination with iridium or making it impossible as seen with diaminoheptane **19** or diaminooctane **20**. Moreover, we examined the impact of carboxy or carbonamide functions on coordination and complex formation. Lower HIE results in specific compounds showed that replacing an amine group with a carboxy derivative reduces deuteration. We propose that this happens because the carboxy anion strongly complexes with iridium, increasing electron density and making CH insertion less likely. Moreover, further

https://doi.org/10.1038/s41467-026-69850-x

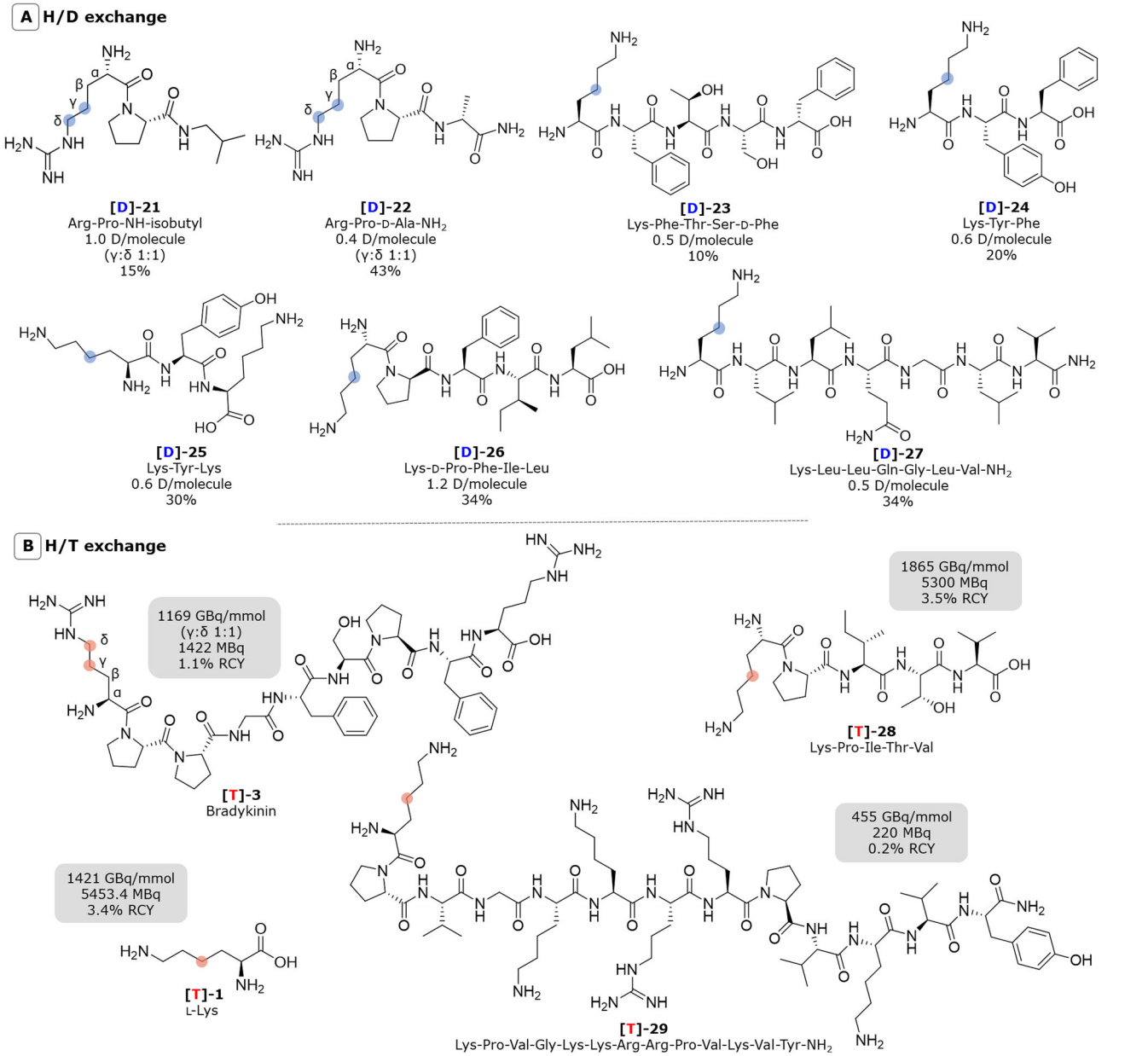

Fig. 5 | HIE on complex peptides. A Deuterium labeling of peptides (blue dot). Conditions for **[D]–21** and **[D]–22**: 0.02 mmol substrate, 2.5 mol% $[Ir(COD)Cl]_2$, 5 mol% ligand **L11**, Borax/HCl buffer pH 9, 90 °C, 17 h. Conditions for **[D]–23** to **[D]–27**: 0.02 mmol substrate, 2.5 mol% $[Ir(COD)Cl]_2$, 5 mol% ligand **L11**, Borax/HCl buffer pH 9, 90 °C, 1 h followed by second addition of 2.5 mol% $[Ir(COD)Cl]_2$ and 5 mol % ligand **L11**. The reaction was left running for at 90 °C for 1 h. **B** Tritium labeling of amino acids and peptides (red dot). Conditions: optimized for each substrate, detailed information in Section 9, pages 141–182 of Supplementary Information).

investigation was carried out on the different energies between hydroxy and amino-mediated coordination in the catalytic system. One striking difference was identified, however, and this concerns the elimination of water from **E** to form the reactant complex **F**. While this step is exergonic (−4.1 kcal/mol) for amino, it is endergonic for hydroxy (+3.0 kcal/mol). We explain this with a stronger coordinating ability for NH_2 compared to OH where excess of electrons makes water leaving more feasible. Furthermore, this is supported further by the finding that the formation of insertion product **G** requires more energy for NH_2 (+13.7 kcal/mol) compared to OH (+12.2 kcal/mol). On the other hand, we found that the regioselectivity in pincer-type species is not affected by electronics, but most probably due to intrinsic geometric constraints. Lysine and arginine compete for iridium coordination at their alpha amino- or carboxy groups. The HIE reaction involves key processes like iridium substrate complexation, CH activation, and substrate exchange at the catalyst sphere, making it difficult to predict the most influential parameter due to complex kinetic and energetic factors. This challenge is significantly greater for larger peptides.

To study the scope of the method, we have performed HIE reactions on peptides **21**–**27**, containing 2-7 different amino acids (Fig. 5A). In full alignment with the results in Fig. 3, we found deuteration only in the γ-position of the *N*-terminal lysine (**23**–**27**) with up to 1.2 D/molecule. For small peptides containing *N*-terminal arginine (**21**–**22**), we observed deuteration up to 1.0 D/molecule in the γ- and δ-positions in a 1:1 ratio. Due to the complexity of the ^{1}H-NMR spectra of several peptides, the quantitative analysis of deuteration was done by HR-MS. Nevertheless, we confirmed the labeling position with deuterium NMR. Under the basic reaction conditions deamidation can occur if

asparagine or glutamine are present in the peptide. However, in some cases (e.g., compound **27**), glutamine was stable. Furthermore, analysis of the crude deuteration reaction of bradykinin **3**, showed only low decomposition side products (Figures S64, S65, page 68 of Supplementary Information). Therefore, to transfer the deuteration method to tritium, the reactions were optimized at low pressure (100–300 mbar) with 8–10 equiv. of deuterium in a pressure-controlled manifold system (Table S12, page 140 of Supplementary Information). Finally, the tritium reactions (with 130–149 GBq tritium gas) yielded the corresponding peptides in a single reaction step with specific activities of 455–1865 GBq/mmol (corresponding to up to 1.7/T molecule). Highly sensitive tritium NMR experiments demonstrated the high selectivity of the method on bradykinin **3** and in complex peptides **28-29** with up to 13 amino acids (Fig. 5B). Interestingly, HIE reactions with deuterium or tritium showed no significant difference in the hydrogen isotope exchange outcome. This is in line with our studies of the kinetic isotope effect with lysine **1** at 90 °C (Table S13, pages 183–184 of Supplementary Information). We calculated the K_i for the H/D exchange to be close to 1 (1.24 precisely). We propose that under the same reaction conditions, the K_i of H/T exchange is not significantly increased, which makes the deuteration reactions suitable simulations for later tracer reactions with tritium.

We have developed a selective HIE method in buffers to introduce deuterium and tritium into unprotected oligopeptides. Through this achievement, radioactive tracer molecules can be produced in a single step with specific activities of up to 1865 GBq/mmol. The labeling positions in lysine and arginine are non-activated and potentially metabolically stable, opening the possibility to study the behavior of labeled complex peptide-based drugs in in vitro or in vivo experiments in the future. This is particularly interesting as isotopically labeled biologics are often overlooked, despite these larger biologics becoming increasingly prevalent in the pharmaceutical industry and serving as life-changing treatments for patients. Furthermore, we have gained insights into the complexation mechanism of the in situ formed catalytic system. DFT calculations revealed the complexation of only one phosphine ligand and the protective nature of the substrate, which prevents heterogeneous metal particle formation.

Methods

Detailed methods for reaction optimization, HIE reactions and data analysis can be found in the Supplementary Information document with their related.

Analytical methods

LC-MS spectra were obtained on Agilent 1200 Series (Agilent Technologies), Column: Luna C18(2) 10 × 2 mm, particle size: 5 μm, Mobile phase A: H_2O + 0.05% TFA, Mobile phase B: ACN + 0.05% TFA, Flow rate: 0.5 mL/min, Detection: UV 254 nm and UV 210 nm.

HR-MS spectra were obtained on a Vanquish (Thermo Fisher) couple with a Bruker Compact QTOF, Column: CSH Peptide C18-N11, 150 × 2.1 mm, particle size: 1.7 μm, Mobile phase A: H_2O/ACN/TFA 900:100:0.5, Mobile phase B: H_2O/ACN/TFA 100:900:0.375, Flow rate: 0.25 mL/min, Detection: UV 10 nm, UV 220 nm, UV 254 nm and UV 280 nm.

Purification of peptides done by RP-HPLC, Column: HyPURITY C18 150 × 21.2 mm, particle size: 5 μm, Mobile phase A: H_2O + 0.05% TFA, Mobile phase B: ACN + 0.05% TFA, Detection: UV 210 nm.

Stability test run by UHPLC. UHPLC spectra were obtained on a Vanquish instrument from Thermo Fischer Scientific, Column: Waters Acquity Peptide CSH 130 C18 150 × 2.1 mm, particle size: 1.7 μm, Mobile phase A: H_2O/ACN/TFA 900:100:0.5, Mobile phase B: H_2O/ACN/TFA 100:900:0.375, Flow rate: 0.5 mL/min, Detection: UV 220 nm and radiodetection.

^{1}H NMR, ^{31}P NMR, deuterium ^{2}H NMR and tritium ^{3}H NMR spectra were obtained on Bruker 300 UltraShieldTM spectrometer (Bruker BioSpin AG). The chemical shifts (δ) are expressed in ppm and are adapted to the proton signal of the respective solvent. The blue dots reported in the chemical structures as well as the blue arrows reported in the NMR spectra indicate the position(s) of hydrogen-deuterium exchange and are determined by ^{2}H NMR run in non-deuterated solvent. For determination of NMR yields, a 39 mM stock solution of maleic acid (purchased from Sigma-Aldrich) in D_2O was prepared. Each sample was solubilized in 0.7 mL of the prepared solution and analyzed by ^{1}H NMR. All spectra were recorded at room temperature.

pH was measured using the Orion Star A211 pH meter (Thermo Fisher Scientific), and the pH meter was calibrated with pH 4/7/10 technical pH buffer solutions (VWR Chemicals).

General method for HIE reactions

A 6 mM stock solution of catalyst $[Ir(COD)Cl]_2$ and a 30 mM stock solution of ligand **L11** were prepared using dioxane as solvent.

The substrate (0.02 mmol, 1 equiv.) was dissolved in 3 mL of Borax/HCl Buffer pH 9, catalyst $[Ir(COD)Cl]_2$ (2.5 mol%, 0.025 equiv.) and ligand **L11** (5 mol%, 0.05 equiv.) were dispensed as the previously prepared stock solution. A stirring bar was added to each reaction flask, which was closed properly and connected to the gas inlet. The flask was evacuated until slight bubbling of the solution and then refilled with deuterium gas. This procedure was repeated three times. The reaction was stirred under D_2 atmosphere (100 equiv.) at 90 °C for 1 h. For some of the L-Lys containing complex peptides after 1 h, catalyst (2.5 mol%, 0.025 equiv.) and ligand **L11** (5 mol%, 0.05 equiv.) were dispensed in 0.5 mL of dioxane and added to the reaction mixture, which was left stirring for another 1 h. For L-Arg and peptides where this amino acid is contained, the reaction time was prolonged to 17 h. The reaction mixture was filtered through a syringe filter (0.45 μm) and one aliquot was analyzed by LC-MS. Additionally, water was removed by lyophilization. The filtered or purified sample was analyzed by ^{1}H and ^{2}H NMR.

Data availability

All data generated or analyzed during this work are reported in the main text of the article and its compiled Supplementary Information document with their related references. Source data are provided with this paper. All data are available from the corresponding author upon request. Source data are provided with this paper.

References

1. Elmore, C. S. & Bragg, R. A. Isotope chemistry: a useful tool in the drug discovery arsenal. *Bioorg. Med. Chem. Lett.* **25**, 167–171 (2015).
2. Derdau, V. et al. The future of (Radio)-labeled compounds in research and development of the life science industry. *Angew. Chem. Int. Ed.* **62**, e202306019 (2023).
3. Di Martino, R. M. C., Maxwell, B. D. & Pirali, T. Deuterium in drug discovery: progress, opportunities and challenges. *Nat. Rev. Drug. Discov.* **22**, 562–584 (2023).
4. Isin, E. M., Elmore, C. S., Nilsson, G. N., Thompson, R. A. & Weidolf, L. Use of radiolabeled compounds in drug metabolism and pharmacokinetic studies. *Chem. Res. Toxicol.* **25**, 532–542 (2012).
5. Neufeld, J. D., Wagner, M. & Murrell, J. C. Who eats what, where and when? Isotope-labeling experiments are coming of age. *ISME J.* **1**, 103–110 (2007).
6. Masson, G. R. et al. Recommendations for performing, interpreting and reporting hydrogen deuterium exchange mass spectrometry (HDX-MS) experiments. *Nat. Methods* **16**, 595–602 (2019).
7. Edelmann, M. R. Radiolabelling small and biomolecules for tracking and monitoring. *RSC Adv.* **12**, 32383 (2022).
8. Zhao, D., Petzold, R., Yan, J., Muri, D. & Ritter, T. Tritiation of aryl thianthrenium salts with a molecular palladium catalyst. *Nature* **600**, 444–449 (2021).
9. Urquhart, L. Top companies and drugs by sales in 2021. *Nat. Rev. Drug Discov.* **21**, 251 (2022).

10. Edelmann, M. et al. Tritium labeling of antisense oligonucleotides via different conjugation agents. *AAPS Open* **7**, Article 4 (2021).
11. Yang, X., Ben, H. & Ragauskas, A. J. Recent advances in the synthesis of deuterium-labeled compounds. *Asian J. Org. Chem.* **10**, 2473–2485 (2021).
12. Atzrodt, J., Derdau, V., Kerr, W. J. & Reid, M. C–H functionalisation for hydrogen isotope exchange. *Angew. Chem. Int. Ed.* **57**, 3022–3047 (2018).
13. Kopf, S. et al. Recent developments for the deuterium and tritium labeling of organic molecules. *Chem. Rev.* **122**, 6634–6718 (2022).
14. Li, W. et al. Scalable and selective deuteration of (hetero)arenes. *Nat. Chem.* **14**, 334–341 (2022).
15. Prakash, G., Paul, N., Oliver, G. A., Werz, D. B. & Maiti, D. C–H deuteration of organic compounds and potential drug candidates *Chem. Soc. Rev.* **51**, 3123 (2022).
16. Yu, R. P., Hesk, D., Rivera, N., Pelczer, I. & Chirik, P. J. Iron-catalysed tritiation of pharmaceuticals. *Nature* **529**, 195–199 (2016).
17. Kang, Q.-K. & Shi, H. Catalytic hydrogen isotope exchange reactions in late-stage functionalization. *Synlett* **33**, 329 (2021).
18. Li, N., Li, Y., Wu, X., Zhu, C. & Xie, J. Radical deuteration. *Chem. Soc. Rev.* **51**, 6291 (2022).
19. Zhou, R., Ma, L., Yang, X. & Cao, J. Recent advances in visible-light photocatalytic deuteration reactions. *Org. Chem. Front.* **8**, 426 (2021).
20. Lepron, M. et al. Nanocatalyzed Hydrogen Isotope Exchange. *Acc. Chem. Res.* **54**, 1465 (2021).
21. Vang, Z. P., Hintzsche, S. J. & Clark, J. R. Catalytic Transfer Deuteration and Hydrodeuteration: EmergingTechniques to Selectively Transform Alkenes and Alkynes to Deuterated Alkanes. *Chem. Eur. J.* **27**, 9988 (2021).
22. Cernak, T., Dykstra, K. D., Tyagarajan, S., Vachal, P. & Krska, S. W. The medicinal chemist's toolbox for late-stage functionalization of drug-like molecules. *Chem. Soc. Rev.* **45**, 546–576 (2016).
23. Wang, P. et al. Ligand-accelerated non-directed C–H functionalization of arenes. *Nature* **551**, 489–493 (2017).
24. Guillemard, L., Kaplaneris, N., Ackermann, L. & Johansson, M. J. Late-stage C–H functionalization offers new opportunities in drug discovery. *Nat. Rev. Chem.* **5**, 522–545 (2021).
25. Castellino, N. J., Montgomery, A. P., Danon, J. J. & Kassiou, M. Late-stage functionalization for improving drug-like molecular properties. *Chem. Rev.* **123**, 8127–8153 (2023).
26. Berger, F. et al. Site-selective and versatile aromatic C–H functionalization by thianthrenation. *Nature* **567**, 223–228 (2019).
27. Valero, M. & Derdau, V. Highlights in C(sp^3)-hydrogen isotope exchange. *J. Label. Compd. Radiopharm.* **63**, 266–280 (2020).
28. Stork, C. M. et al. Hydrogen isotope exchange by homogeneous iridium catalysis in aqueous buffers with deuterium or tritium gas. *Angew. Chem. Int. Ed.* **62**, e202301512 (2023).
29. Martinelli, E. et al. Pegylated phosphine ligands in iridium(I) catalyzed hydrogen isotope exchange reactions in aqueous buffers. *Chem. Eur. J.* **30**, e202402038 (2024).
30. Bolleddula, J. et al. Biotransformation and bioactivation reactions of alicyclic amines in drug molecules. *Drug Metab. Rev.* **46**, 379–419 (2014).
31. Murai, Y. et al. Rapid and controllable hydrogen/deuterium exchange on aromatic rings of α-amino acids and peptides. *Eur. J. Org. Chem.* **23**, 5111–5116 (2013).
32. Park, S. et al. Simple and efficient enantioselective α-deuteration method of α-amino acids without external chiral sources. *JACS Au* **4**, 2246–2251 (2024).
33. Taglang, C. et al. Activation using ruthenium nanocatalysts. *Angew. Chem., Int. Ed.* **54**, 10474–10477 (2015).
34. Martinez-Prieto, L. M. et al. Monitoring of nanoparticle reactivity in solution: interaction of l-lysine and Ru nanoparticles probed by chemical shift perturbation parallels regioselective H/D exchange. *Chem. Commun.* **53**, 5850–5853 (2017).
35. Zuluaga-Villamil, A. et al. N-heterocyclic carbene-based iridium and ruthenium/iridium nanoparticles for the hydrogen isotope exchange reaction through C–H bond activations. *Organometallics* **41**, 3313–3319 (2022).
36. Michelotti, A., Rodrigues, F. & Roche, M. Development and scale-up of stereoretentive α-deuteration of amines. *Org. Process Res. Dev.* **21**, 1741–1744 (2017).
37. Kokel, A., Kadish, D. & Török, B. Preparation of deuterium labeled compounds by Pd/C-Al-D_2O facilitated selective H-D exchange reactions. *Molecules* **27**, 614 (2022).
38. Chatterjee, B., Krishnakumar, V. & Gunanathan, C. Selective α-deuteration of amines and amino acids using D_2O. *Org. Lett.* **18**, 5892–5895 (2016).
39. Takeda, R. et al. Asymmetric synthesis of α-deuterated α-amino acids. *Org. Biomol. Chem.* **15**, 6978–6983 (2017).
40. Valero, M., Weck, R., Güssregen, S., Atzrodt, J. & Derdau, V. Highly selective directed iridium-catalyzed hydrogen isotope exchange reactions of aliphatic amides. *Angew. Chem. Int. Ed.* **57**, 8159–8163 (2018).
41. Loh, Y. Y. et al. Photoredox-catalyzed deuteration and tritiation of pharmaceutical compounds. *Science* **358**, 1182–1187 (2017).
42. Legros, F. et al. Photoredox-mediated hydrogen isotope exchange reactions of amino-acids, peptides, and peptide-derived drugs. *Chem. Eur. J.* **26**, 12738–12742 (2020).
43. Narayan, A. R. H. & Chun, S. W. Biocatalytic, stereoselective deuteration of α-amino acids and methyl esters. *ACS Catal.* **10**, 7413–7418 (2020).
44. Gao, J., Zhou, C. & Hai, Y. Stereoselective biocatalytic α-deuteration of l-amino acids by a pyridoxal 5′-phosphate-dependent mannich cyclase. *ChemBioChem* **24**, e202300561 (2023).
45. Doyon, T. J. & Buller, A. R. Site-selective deuteration of amino acids through dual-protein catalysis. *J. Am. Chem. Soc.* **144**, 7327–7336 (2022).
46. Kerr, W. J., Mudd, R. J., Reid, M., Atzrodt, J. & Derdau, V. Iridium-catalyzed Csp^3-H activation for mild and selective hydrogen isotope exchange. *ACS Catal.* **8**, 10895–10900 (2018).
47. Ellames, G. J., Gibson, J. S., Herbert, J. M., Kerr, W. J. & McNeill, A. H. Deuterium exchange mediated by an iridium–phosphine complex formed in situ. *Tetrahedron Lett.* **42**, 6413–6416 (2001). ***In situ generated ligated iridium catalysts were studied before in HIE in organic media***.
48. Herbert, J. M. Deuterium exchange promoted by iridium complexes formed in situ. *J. Label. Compd. Radiopharm.* **53**, 658–661 (2010).
49. Crabtree, R. Iridium compounds in catalysis. *Acc. Chem. Res.* **12**, 331 (1979).
50. Brown, J. A. et al. Highly active iridium(I) complexes for catalytic hydrogen isotope exchange *Chem. Commun.* **2008**, 1115–1117 (2008).
51. Nilsson, G. N. & Kerr, W. J. The development and use of novel iridium complexes as catalysts for ortho-directed hydrogen isotope exchange reactions. Label. *Compd*. R*adiopharm* **53**, 662 (2010).
52. Cochrane, A. R. et al. Application of neutral iridium(I) *N*-heterocyclic carbene complexes in ortho-directed hydrogen isotope exchange. *J. Label. Compd. Radiopharm.* **56**, 451 (2013).
53. Cross, P., Herbert, J., Kerr, W., McNeill, A., Paterson, L. Isotopic labelling of functionalised arenes catalysed by Ir(I) species of the [(COD)Ir(NHC)(py)]PF_6 complex class *Synlett* **27**, 111 (2015).
54. Kerr, W. J., Knox, G. J., Reid, M. & Tuttle, T. Catalyst design in C–H activation: a case study in the use of binding free energies to rationalise intramolecular directing group selectivity in iridium catalysis *Chem. Sci* **12**, 6747–6755 (2021).
55. Cochrane, A. R. et al. Practically convenient and industrially-aligned methods for iridium-catalysed hydrogen isotope exchange processes. *Org. Biomol. Chem.* **12**, 3598 (2014).

56. Kennedy, A. R., Kerr, W. J., Moir, R. & Reid, M. Anion effects to deliver enhanced iridium catalysts for hydrogen isotope exchange processes. *Org. Biomol. Chem.* **12**, 7927 (2014).
57. Kerr, W. J. et al. Hydrogen isotope exchange with highly active iridium(I) NHC/phosphine complexes: a comparative counterion study. *J. Label. Compd. Radiopharm.* **59**, 601 (2016).
58. Brown, J. A. et al. The synthesis of highly active iridium (I) complexes and their application in catalytic hydrogen isotope exchange. *Adv. Synth. Catal.* **356**, 3551 (2014).
59. Timofeeva, D. S., Lindsay, D. M., Kerr, W. J. & Nelson, D. J. A quantitative empirical directing group scale for selectivity in iridium-catalysed hydrogen isotope exchange reactions. *Catal Sci. Technol.* **10**, 7249–7255 (2020).
60. Timofeeva, D. S., Lindsay, D. M., Kerr, W. J. & Nelson, D. J. Are rate and selectivity correlated in iridium-catalysed hydrogen isotope exchange reactions? *Catal. Sci. Technol.* **11**, 5498 (2021).
61. Kerr, W. J. et al. Iridium-catalysed ortho-H/D and-H/T exchange under basic conditions: C–H activation of unprotected tetrazoles. *Chem. Commun.* **52**, 6669 (2016).
62. Kerr, W. J., Reid, M., Tuttle, T. Iridium-catalyzed C–H activation and deuteration of primary sulfonamides: an experimental and computational study. *ACS Catal.* **5**, 402 (2015).
63. Kerr, W. J., Mudd, R. J., Reid, M., Atzrodt, J. & Derdau, V. Iridium-catalyzed Csp^3–H activation for mild and selective hydrogen isotope exchange. *ACS Catal.* **8**, 10895 (2018).
64. Knight, N. M. L. et al. Iridium-catalysed C(sp^3)–H activation and hydrogen isotope exchange via nitrogen-based carbonyl directing groups. *Adv. Synth. Catal.* **366**, 2577 (2024).
65. Kerr, W. J., Reid, M. & Tuttle, T. Iridium-catalyzed formyl-selective deuteration of aldehydes *Angew. Chem. Int. Ed.* **56**, 7808 (2017).
66. Kerr, W. J. et al. Site-selective deuteration of N-heterocycles via iridium-catalyzed hydrogen isotope exchange. *ACS Catal.* **7**, 7182 (2017).
67. Heys, R. et al. Investigation of $[IrH_2(Me_2CO)_2(PPh_3)_2]BF_4$ as a catalyst of hydrogen isotope exchange of substrates in solution. *J. Chem. Soc., Chem. Commun.* **9**, 680–681 (1992).
68. Heys, J. R., Shu, A. Y. L., Senderoff, S. G. & Phillips, N. M. Deuterium exchange labelling of substituted aromatics using $[IrH_2(Me_2CO)_2(PPh_3)_2]BF_4$. *J. Label. Compd. Radiopharm.* **33**, 431–438 (1993).
69. Shu, A. Y. L., Chen, W. & Heys, J. R. Organoiridium catalyzed hydrogen isotope exchange: ligand effects on catalyst activity and regioselectivity. *J. Organomet. Chem.* **524**, 87–93 (1996).
70. Chen, W. et al. Direct tritium labeling of multifunctional compounds using organoiridium catalysis. *J. Label. Compd. Radiopharm.* **39**, 291–298 (1997).
71. Shu, A. Y. L. et al. Direct tritium labeling of multifunctional compounds using organoiridium catalysis. *J. Label. Compd. Radiopharm.* **42**, 797–807 (1999).
72. Shu, A. Y. L. & Heys, J. R. Direct, efficient and selective tritiations of paclitaxel and photoaffinity toxoids. *Tetrahedron Lett.* **41**, 9015–9019 (2000).
73. Kramp, H. et al. In-situ generated iridium nanoparticles as hydride donors in photoredox-catalyzed hydrogen isotope exchange reactions with deuterium and tritium gas. *Angew. Chem. Int. Ed.* **62**, e202308983 (2023).
74. Daniel-Bertrand, M. et al. Multiple site hydrogen isotope labeling of pharmaceuticals. *Angew. Chem. Int. Ed.* **59**, 21114–21120 (2020).
75. Valero, M. et al. NHC-ligated iridium nanoparticles as novel catalysts in hydrogen isotope exchange reactions. *Angew. Chem. Int. Ed.* **59**, 3517–3522 (2020).
76. Zhao, Y. & Truhlar, D. G. The M06 suite of density functionals for main group thermochemistry, thermochemical kinetics, noncovalent interactions, excited states, and transition elements: two new functionals and systematic testing of four M06-class functionals and 12 other functionals. *Theor. Chem. Acc.* **120**, 215–241 (2008).
77. Gusev, D. G. & Berke, H. Hydride fluxionality in transition metal complexes: an approach to the understanding of mechanistic features and structural diversities. *Chem. Ber.* **129**, 1143–1155 (1996).

Acknowledgements

We thank Claudia Loewe for assistance with mass spectrometry and liquid scintillation analyses related to ^{3}H-labeling experiments. The authors want to thank Dr. Anika Tarasewicz (Sanofi Germany) for proof reading of the manuscript.

Author contributions

E.M. performed the experiments, synthesized and characterized the molecules, analyzed the data and discussed the results. R.W. performed the radioactive experiments. S.G. performed the DFT calculations. V.D. organized the funding, conceptualized and directed the project. All authors prepared the manuscript. E.M. is a participant in the EU ITN ISOBIOTICS consortium. The ISOBIOTICS project has received funding from the European Union's Horizon 2020 research and innovation program under the Marie Skłodowska-Curie grant agreement No. 101072780.

Competing interests

All authors are employees of Sanofi Germany and may hold shares or options of the company.

Additional information

Supplementary information The online version contains supplementary material available at https://doi.org/10.1038/s41467-026-69850-x.

Correspondence and requests for materials should be addressed to Volker Derdau.

Peer review information *Nature Communications* thanks the anonymous reviewer(s) for their contribution to the peer review of this work. A peer review file is available.